Available online at www.sciencedirect.com
SCIENCE DIRECT®
Journal of Computational Physics 203 (2005) 379–385
JOURNAL OF COMPUTATIONAL PHYSICS
www.elsevier.com/locate/jcp

Short Note

Hyperviscosity for shock-turbulence interactions

Andrew W. Cook *, William H. Cabot

Lawrence Livermore National Laboratory, Livermore, CA 94550, USA

Received 1 March 2004; received in revised form 20 August 2004; accepted 26 September 2004
Available online 5 November 2004

Abstract

An artificial viscosity is described, which functions as an effective subgrid-scale model for both high and low Mach number flows. The model employs a bulk viscosity for treating shocks and a shear viscosity for treating turbulence. Each of the viscosities contains an empirical constant; however, the constants do not require adjustment from flow to flow. A polyharmonic operator, applied to the strain rate, imparts spectral-like behavior to the model, thus eliminating the need for *ad hoc* limiters and/or "dynamic procedures" to turn off the model in smooth regions. The model gives excellent results for Shu's problem, Noh's problem and decaying turbulence.

Keywords: Artificial viscosity; Subgrid-scale model; Shock capturing; Turbulence

Over half a century ago, von Neumann and Richtmyer [1] introduced the idea of adding artificial viscosity to the Euler equations in order to help stabilize shock calculations. The ideas of von Neumann, regarding artificial viscosity, influenced Smagorinsky in his development of a subgrid-scale model designed to match the Kolmogorov spectrum for atmospheric turbulence [2,3]. Since that time, numerous artificial viscosity formulations have been proposed for simulating both shocks and turbulence [4–10]. Over the years however, a rift has developed between shock capturing (monotonicity-preserving) and turbulence-capturing (large-eddy simulation) methods. Artificial viscosities for shock capturing typically depend on sound speed, which makes them unsuitable for low Mach number flows. On the other hand, subgrid-scale models, customized for incompressible turbulence, usually fail to capture shocks in a monotonic fashion. A unified treatment of flow discontinuities and turbulent subgrid scales was previously pursued by Adams and Stolz [11], who employed a regularized approximate deconvolution technique to simulate shocks in one dimension. The purpose of this paper is to introduce an artificial viscosity suitable for computing

* Corresponding author. Tel.: +1 510 423 2856; fax: +1 510 423 0925.
E-mail address: awcook@llnl.gov (A.W. Cook).

0021-9991/$ - see front matter
doi:10.1016/j.jcp.2004.09.011

shock-turbulence interactions. This is accomplished by extending the model of Cook and Cabot [10] to multiple dimensions.

The Navier–Stokes equations for compressible flow of an ideal gas, with constant specific heats, are (underline denotes tensor):

$$\dot{\rho} + \nabla \cdot \rho \mathbf{u} = 0, \tag{1}$$

$$\dot{\mathbf{m}} + \nabla \cdot (\rho \mathbf{u}\mathbf{u} + p\underline{\boldsymbol{\delta}} - \underline{\boldsymbol{\tau}}) = 0, \tag{2}$$

$$\dot{E} + \nabla \cdot [E\mathbf{u} + (p\underline{\boldsymbol{\delta}} - \underline{\boldsymbol{\tau}}) \cdot \mathbf{u} + \mathbf{q}] = 0, \tag{3}$$

$$p = (\gamma - 1)\rho e, \tag{4}$$

where ρ is density, $\mathbf{u}$ is velocity, $\mathbf{m} = \rho u$ is momentum, p is pressure, $\underline{\boldsymbol{\delta}}$ is the unit tensor, $E = \rho(e + \mathbf{u} \cdot \mathbf{u}/2)$ is total energy, e is specific internal energy and $\gamma = c_p/c_v$ is the ratio of specific heats. The viscous stress tensor, $\underline{\boldsymbol{\tau}}$, is given by

$$\underline{\boldsymbol{\tau}} = \mu(2\underline{\mathbf{S}}) + (\beta - \tfrac{2}{3}\mu)(\nabla \cdot \mathbf{u})\underline{\boldsymbol{\delta}}, \tag{5}$$

where μ is dynamic (shear) viscosity, β is bulk viscosity and $\underline{\mathbf{S}}$ is the symmetric strain rate tensor

$$\underline{\mathbf{S}} = \tfrac{1}{2}(\nabla \mathbf{u} + \mathbf{u}\nabla), \tag{6}$$

where $\mathbf{u}\nabla$ denotes the transpose of $\nabla\mathbf{u}$. The conductive heat flux vector, $\mathbf{q}$, is given by Fourier's law,

$$\mathbf{q} = -\sigma \nabla T, \tag{7}$$

where σ is thermal conductivity and $T = (\gamma - 1)e/R$ is temperature (with $R = c_p - c_v$ being the gas constant). At high Mach numbers and high Reynolds numbers, the Navier–Stokes equations admit scales of motion too small to practically resolve on numerical grids. A key problem in simulating such flows is how to properly remove energy above the Nyquist wavenumber without corrupting the remaining flow. We will demonstrate how an artificial viscosity with spectral-like behavior can accomplish this objective.

Our approach is to add grid-dependent components to the viscosity coefficients, i.e., $\mu = \mu_f + \mu_\Delta$ and $\beta = \beta_f + \beta_\Delta$ are used in (5), where the f subscript denotes physical viscosity and the Δ subscript denotes artificial viscosity. The grid-dependent shear and bulk viscosities can be considered subgrid-scale model coefficients for the convective portions of the filtered momentum and energy equations. Due to the necessarily-limited scope of this Short Note, additional subgrid-scale terms in the filtered energy equation are neglected, e.g., pressure-dilatation. Also, potential benefits of including subgrid-scale heat transport via a grid-dependent thermal conductivity (σ_Δ) are not considered here.

Spectral-like models for μ_Δ and β_Δ are

$$\mu_\Delta = C_\mu^r \eta_r, \qquad \beta_\Delta = C_\beta^r \eta_r, \quad \eta_r = \rho \Delta^{(r+2)} \overline{|\nabla^r S|}, \quad r = 2, 4, 6, \ldots, \tag{8}$$

where C_μ^r and C_β^r are user-specified constants, Δ is local grid spacing (cube-root of cell volume) and $S = (\underline{\mathbf{S}}:\underline{\mathbf{S}})^{1/2}$ is the magnitude of the strain rate tensor. The polyharmonic operator, $\nabla^r S$, denotes a series of Laplacians, e.g., $r = 4$ corresponds to the biharmonic operator, $\nabla^4 S = \nabla^2(\nabla^2 S)$. The overbar ($\overline{f}$) denotes a truncated-Gaussian filter, defined as

$$\overline{f}(\mathbf{x}) = \int_{-L}^{L} G(|\mathbf{x} - \boldsymbol{\xi}|; L) f(\boldsymbol{\xi})\, \mathrm{d}^3\xi, \tag{9}$$

where

$$G(\zeta; L) = \frac{\mathrm{e}^{-6\zeta^2/L^2}}{\int_{-L}^{L} \mathrm{e}^{-6\zeta^2/L^2}\, \mathrm{d}\zeta}, \quad L = 4\Delta. \tag{10}$$

This filter eliminates cusps introduced by the absolute value operator, which in turn, ensures that the viscosities are positive definite. In the present work, (9) is approximated along each grid line as

$$\overline{f}_j = \frac{3565}{10,368} f_j + \frac{3091}{12,960}(f_{j-1} + f_{j+1}) + \frac{1997}{25,920}(f_{j-2} + f_{j+2}) + \frac{149}{12,960}(f_{j-3} + f_{j+3}) + \frac{107}{103,680}(f_{j-4} + f_{j+4}). \tag{11}$$

The transfer function associated with this filter stencil closely matches a Gaussian. In practice, the model does not appear sensitive to the particular integration rule chosen for (9).

Eq. (8) corresponds to Smagorinsky's model if $r = C_\beta^r = 0$ and $L \to 0$ in the limit. Inclusion of the bulk viscosity term is the key to capturing shocks without destroying vorticity, i.e., β_Δ can be made large (to smooth shocks) without impacting small-scale turbulence in regions where $\nabla \cdot \mathbf{u} \approx 0$. Additionally, by setting $r > 0$, the viscosity keys directly on the ringing, rather than indirectly on gradients. This eliminates the need for limiters and switches to turn off β_Δ in special cases, e.g., expansion, isentropic compression, rigid rotation, etc. It also removes the need for a "dynamic procedure" [12] to turn off μ_Δ in regions of uniform shear. The polyharmonic operator has some theoretical justification in that it imparts a high-wavenumber bias to the artificial viscosity, thus approximating the cusp in the Heisenberg–Kraichnan spectral viscosity [13,14] for isotropic turbulence. Cook and Cabot [10] have demonstrated, for smooth flow in one dimension, that higher convergence rates can be achieved by increasing r. However, larger values of r require higher-order approximations for the derivatives. Anticipating implementation of the model on nonuniform grids, where only a single Laplacian is feasible, we chose $r = 2$ for the current simulations and set $C_\mu^2 = 0.025$ and $C_\beta^2 = 5$. Recommended values for the empirical coefficients with $r = 4$ are $C_\mu^4 = 0.002$ and $C_\beta^4 = 1$. These values were chosen based on fits to a wide variety of shock and turbulence test problems.

A potential concern for hyperviscosity models such as (8) is that they change the type of the underlying partial differential equation (PDE), since (8) constitutes a higher-order perturbation [11]. Accordingly, for initial-boundary value problems, boundary data imposed for the unperturbed PDEs may lead to an ill-posed problem. In this Short Note, we consider only problems with constant or periodic boundaries. For periodic problems, Cook and Cabot [10] have demonstrated that solutions to the modified PDEs converge to the correct weak solutions.

In evaluating the model, it is desirable to use a numerical scheme with low truncation error and minimal implicit dissipation, which would otherwise compete with $\underline{\tau}$. Therefore, we use Fourier transforms to compute spatially-periodic derivatives, a tenth-order compact scheme [15] for nonperiodic derivatives, and a fourth-order Runge–Kutta (RK4) scheme (with CFL = 1) for temporal integration. De-aliasing is accomplished by applying either a 2/3-wavenumber truncation (periodic directions) or eighth-order compact filter (non-periodic directions) to the conserved variables after each RK4 substep. The compact filter stencil is

$$\beta\hat{f}_{j-2} + \alpha\hat{f}_{j-1} + \hat{f}_j + \alpha\hat{f}_{j+1} + \beta\hat{f}_{j+2} = af_j + \frac{b}{2}(f_{j-1} + f_{j+1}) + \frac{c}{2}(f_{j-2} + f_{j+2}) + \frac{d}{2}(f_{j-3} + f_{j+3}) + \frac{e}{2}(f_{j-4} + f_{j+4}), \tag{12}$$

where $\hat{f}$ is the filtered variable and

$$\alpha = 0.66624, \quad \beta = 0.16688, \quad a = 0.99965, \quad \frac{b}{2} = 0.66652, \tag{13}$$

$$\frac{c}{2} = 0.16674, \quad \frac{d}{2} = 4 \times 10^{-5}, \quad \frac{e}{2} = -5 \times 10^{-6}. \tag{14}$$

The transfer function of this filter provides a fairly sharp high-wavenumber cut-off. Further details of the numerical scheme are provided in Cook and Cabot [10]. The spectral/compact filtering not only provides

space for higher wavenumbers (generated by nonlinear terms) to temporarily exist, it also prevents μ_Δ and β_Δ from becoming too large. For example, without the spectral/compact filter, β_Δ can become extremely large in the vicinity of strong shocks, thus driving the viscously-stable timestep to zero and bringing the simulation to a halt. The de-aliasing filter constitutes an additional kinetic-energy sink; however, if the filter is spectrally sharp, e.g., Fourier truncation, then the rate of energy removal will not depend on the frequency of filtering, i.e., filtering a signal a second time leaves the solution unchanged. The simulations reported here were all performed on uniform Cartesian grids, where $\Delta x = \Delta y = \Delta z = \Delta$. Except where otherwise noted, μ_f, β_f and σ were all set to zero in each test problem.

The first test case is the Shu–Osher problem, a canonical model of a one-dimensional shock-turbulence interaction [16]. The initial conditions are: $\rho = 3.857143$, $p = 10.33333$ and $u = 2.629369$ for $x < -4$, and $\rho = 1 + 0.2\sin(5x)$, $p = 1$ and $u = 0$ for $x \geqslant -4$, with $\gamma = 1.4$. As the shock propagates into the sinusoidal density field, it leaves a steeply-oscillating flow in the post-shock region. Fig. 1 displays results of the hyperviscosity model for comparison with the results of Adams and Stolz [11]. The slight mismatch near $x = -3$ is a startup error. The model removes nonphysical oscillations surrounding the shock without attenuating physical oscillations in the shock's wake.

The second test case is the spherical Noh implosion [17]. The initial conditions are: $\rho = 1$, $p = 0$ and $\mathbf{u}$ = unit vector directed toward origin, with $\gamma = 5/3$. In this problem, an infinite-strength shock expands outward from the origin at a constant velocity of 1/3. The objective here is to test the ability of a scheme to preserve spherical symmetry and produce the correct entropy jump for adiabatic shock compression. In some sense, this problem represents a worst-case scenario for artificial viscosity methods, since any additional heating from the dissipation function results in reduced compression. In Fig. 2, density is plotted versus radius at two different angles to the grid. The drop-off at small radius is the well-known "wall heating" problem [18], which arises from the singularity in the initial velocity field. Without the hyperviscosity model, the simulation becomes numerically unstable and fails to complete. As indicated by the coincidence of the on-axis and off-axis density curves, the model is insensitive to grid orientation, i.e., it maintains spherical symmetry, albeit with a slight discrepancy close to the origin. Regarding the entropy jump, the

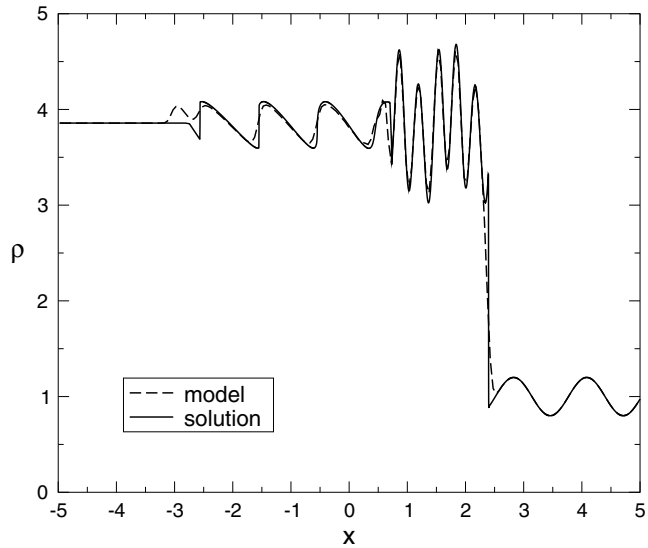

Fig. 1. Density field for the Shu–Osher problem at $t = 1.8$. The solid curve is the converged solution and the dashed curve is the solution with the hyperviscosity model at a resolution of 200 grid points ($\Delta = 0.05$).

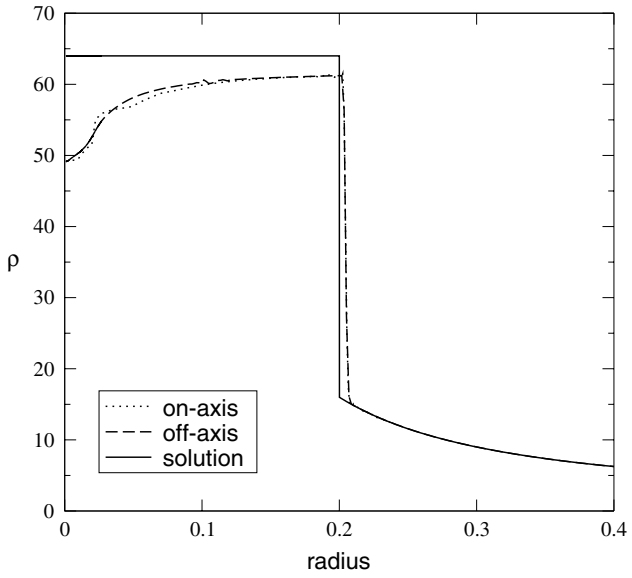

Fig. 2. Density versus radius for Noh's problem at $t = 0.6$. The dotted line is along the z-axis ($\theta = \phi = 0$) and the dashed line is diagonal to the grid ($\theta = \phi = 45°$). The simulation was conducted on an octant of a sphere with $\Delta = 10^{-3}$.

simulated shock does not quite produce the theoretical post-shock density of $\rho = 64$, due to viscous heating. The increased temperature, and hence sound speed, in the compressed region cause the simulated shock to run slightly ahead of the theoretical prediction. The compression ratio is resolution dependent; e.g., for $\Delta = 5 \times 10^{-3}$ and $\Delta = 10^{-3}$ the post-shock density is 55.2 and 61.5, respectively. Therefore, the artificial bulk viscosity method is applicable to very strong shocks, provided sufficient resolution is allocated to the problem.

The third and final test case is the decaying turbulence experiment of Kang et al. [19]. In their experiment, air is blown past an active grid in the Corrsin wind tunnel [20,21], generating near-isotropic turbulence at a Taylor microscale Reynolds number of about 720. An array of four X-wire probes is used to measure velocity at downstream stations: $x/M = 20$, 30, 40 and 48, where $M = 0.152$ m is the shaft spacing of the active grid. The initial conditions for the simulation consist of a triply-periodic velocity field in a 192^3 box, with a kinetic energy spectrum matched to the first 64 wavenumbers of the experimental spectrum at $x/M = 20$. Wavenumbers above 64 are truncated in our simulation in order to match the resolution of the simulations in Kang et al. [19]. Pressure is obtained by solving a Poisson equation with $\nabla \cdot u = 0$. Kinematic viscosity is set to $\nu_f = \mu_f/\rho_{air} = 0.15$ cm^2/s. Simulation time is related to distance downstream using the mean flow velocity, i.e., $x = Ut$, where $U = 11.2$ m/s. Fig. 3 depicts the evolution of the 3-D kinetic energy spectrum, $E(k)$, as well as the decay of turbulent kinetic energy, KE, for the experiment and simulations. The results indicate that the hyperviscosity model provides the correct rate of subgrid-scale energy transfer, resulting in a robust Kolmogorov ($k^{-5/3}$) spectrum and correct rate of energy decay. With no subgrid-scale model, the spectral energy flux is corrupted, as evidenced by the anomalous curvature of the spectrum and too-slow decay of turbulent kinetic energy. It is worth mentioning that Dantinne et al. [8] found qualitatively-similar results using alternative hyperviscosity models in large-eddy simulations of the Comte–Bellot Corrsin experiment.

In summary, we have proposed an artificial bulk viscosity for treating shocks, and an artificial shear viscosity for modeling subgrid-scale turbulence. By adjusting the order of the polyharmonic operator, the viscosities can be strongly weighted toward high wavenumbers, thus imparting spectral-like behavior to

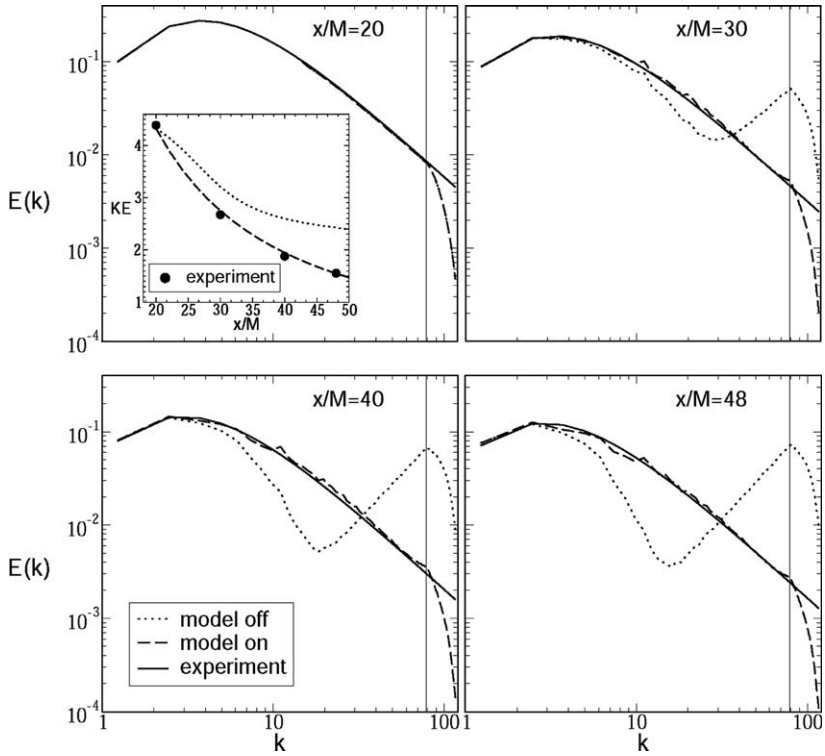

Fig. 3. Evolution of 3D energy spectrum, $E(k)$, for high Reynolds number wind tunnel experiment of Kang et al. [19]. The inset in the first plot shows decay of turbulent kinetic energy (KE). The vertical lines correspond to the 2/3-wavenumber truncation, which serves to de-alias the numerical simulation.

the dissipation. The model is inexpensive and straightforward to implement, and should provide useful means for simulating shock-turbulence interactions.

Acknowledgments

The authors are grateful to Prof. A. Leonard for helpful advice regarding this effort. This work was performed under the auspices of the U.S. Department of Energy by the University of California Lawrence Livermore National Laboratory under contract No. W-7405-Eng-48.

References

[1] J. von Neumann, R.D. Richtmyer, A method for the numerical calculations of hydrodynamical shocks, J. Appl. Phys. 21 (1950) 232–237.
[2] J. Smagorinsky, General circulation experiments with the primitive equations, part I: The basic experiment, Mon. Weather Rev. 91 (1963) 99–152.
[3] J. Smagorinsky, Some Historical Remarks on the Use of Nonlinear Viscosities, Cambridge University Press, 1993, pp. 2–36.
[4] A. Jameson, W. Schmidt, E. Turkel, Numerical simulation of the Euler equations by finite volume methods using Runge–Kutta time stepping schemes, in: AIAA paper 81-1259, AIAA 5th Computations Fluid Dynamics Conference, 1981.
[5] E. Tadmor, Convergence of spectral methods for nonlinear conservation laws, SIAM J. Numer. Anal. 26 (1989) 30–44.

[6] C.K.W. Tam, J.W. Webb, Z. Dong, A study of the short wave components in computational aeroacoustics, J. Comput. Acoust. 1 (1993) 1–30.
[7] A. Misra, D.I. Pullin, A vortex-based subgrid stress model for large-eddy simulation, Phys. Fluids 9 (1997) 2443–2454.
[8] G. Dantinne, H. Jeanmart, G.S. Winckelmans, V. Legat, D. Carati, Hyperviscosity and vorticity-based models for subgrid scale modeling, Appl. Scient. Res. 59 (1998) 409–420.
[9] G.-S. Karamanos, G.E. Karniadakis, A spectral vanishing viscosity method for large-eddy simulations, J. Comput. Phys. 163 (2000) 22–50.
[10] A.W. Cook, W.H. Cabot, A high-wavenumber viscosity for high resolution numerical methods, J. Comput. Phys. 195 (2004) 594–601.
[11] N.A. Adams, S. Stolz, A subgrid-scale deconvolution approach for shock capturing, J. Comput. Phys. 178 (2002) 391–426.
[12] P. Moin, K. Squires, W. Cabot, S. Lee, A dynamic subgrid-scale model for compressible turbulence and scalar transport, Phys. Fluids 3 (1991) 2746–2757.
[13] W. Heisenberg, Zur statistischen theorie der turbulenz, Z. Phys. 124 (1948) 628–657.
[14] R.H. Kraichnan, Eddy viscosity in two and three dimensions, J. Atmos. Sci. 33 (1976) 1521–1536.
[15] S.K. Lele, Compact finite difference schemes with spectral-like resolution, J. Comput. Phys. 103 (1992) 16–42.
[16] C.-W. Shu, S.J. Osher, Efficient implementation of essentially nonoscillatory shock capturing schemes II, J. Comput. Phys. 83 (1989) 32–78.
[17] W.F. Noh, Errors for calculations of strong shocks using an artificial viscosity and an artificial heat flux, J. Comput. Phys. 72 (1987) 78–120.
[18] W.J. Rider, Revisiting wall heating, J. Comput. Phys. 162 (2000) 395–410.
[19] H.S. Kang, S. Chester, C. Meneveau, Decaying turbulence in an active-grid-generated flow and comparisons with large-eddy simulation, J. Fluid Mech. 480 (2003) 129–160.
[20] G. Comte-Bellot, S. Corrsin, The use of a contraction to improve the isotropy of grid-generated turbulence, J. Fluid Mech. 25 (1966) 657–682.
[21] G. Comte-Bellot, S. Corrsin, Simple Eulerian time correlation of full and narrow-band velocity signals in grid-generated 'isotropic' turbulence, J. Fluid Mech. 48 (1971) 273–337.